

# Label-free detection of nucleic acids by turn-on and turn-off G-quadruplex-mediated fluorescence

Jiangtao Ren · Haixia Qin · Jiahai Wang ·  
Nathan W. Luedtke · Erkang Wang · Jin Wang

Received: 12 October 2010 / Revised: 1 December 2010 / Accepted: 5 January 2011 / Published online: 26 January 2011  
© Springer-Verlag 2011

**Abstract** In this study we have used two fluorescent probes, tetrakis(diisopropylguanidino)-zinc-phthalocyanine (Zn-DIGP) and *N*-methylmesoporphyrin IX (NMM), to monitor the reassembly of “split” G-quadruplex probes on hybridization with an arbitrary “target” DNA. According to this approach, each split probe is designed to contain half of a G-quadruplex-forming sequence fused to a variable sequence that is complementary to the target DNA. Upon mixing the individual components, both base-pairing interactions and G-quadruplex fragment reassembly result in a duplex–quadruplex three-way junction that can bind to fluorescent dyes in a G-quadruplex-specific way. The overall fluorescence intensities of the resulting complexes were dependent on the formation of proper base-pairing

interactions in the duplex regions, and on the exact identity of the fluorescent probe. Compared with samples lacking any “target” DNA, the fluorescence intensities of Zn-DIGP-containing samples were lower, and the fluorescence intensities of NMM-containing samples were higher on addition of the target DNA. The resulting biosensors based on Zn-DIGP are therefore termed “turn-off” whereas the biosensors containing NMM are defined as “turn-on”. Both of these biosensors can detect target DNAs with a limit of detection in the nanomolar range, and can discriminate mismatched from perfectly matched target DNAs. In contrast with previous biosensors based on the peroxidase activity of heme-bound split G-quadruplex probes, the use of fluorescent dyes eliminates the need for unstable sensing components ( $H_2O_2$ , hemin, and ABTS). Our approach is direct, easy to conduct, and fully compatible with the detection of specific DNA sequences in biological fluids. Having two different types of probe was highly valuable in the context of applied studies, because Zn-DIGP was found to be compatible with samples containing both serum and urine whereas NMM was compatible with urine, but not with serum-containing samples.

**Electronic supplementary material** The online version of this article (doi:10.1007/s00216-011-4669-0) contains supplementary material, which is available to authorized users.

J. Ren · H. Qin · J. Wang (✉) · E. Wang (✉) · J. Wang (✉)  
State Key Laboratory of Electroanalytical Chemistry,  
Changchun Institute of Applied Chemistry,  
Chinese Academy of Science,  
Changchun, Jilin 130022, China  
e-mail: jhwang@ciac.jl.cn  
e-mail: ekwang@ciac.jl.cn  
e-mail: jin.wang.1@stonybrook.edu

J. Ren · H. Qin  
Graduate School of Chinese Academy of Science,  
Beijing 100039, China

N. W. Luedtke  
Institute of Organic Chemistry, University of Zürich,  
Winterthurerstrasse 190,  
8057 Zürich, Switzerland

J. Wang  
Department of Chemistry and Physics,  
State University of New York at Stony Brook,  
New York, NY 11794-3400, USA

**Keywords** G-quadruplex · Conformational constraint · Split probe · Fluorescent probe

## Introduction

The specific detection of DNA and RNA sequences has attracted widespread efforts aimed at rapid genetic profiling and disease diagnosis [1–7]. Most methods rely on hybridization between probe DNA and a complementary “target” sequence followed by signal amplification and detection by electrochemistry [4–6], colorimetry [1, 2], or fluorescence [7]. Molecular beacons, first reported by Tyagi

and Kramer [8], are dual-labeled oligonucleotides that become more fluorescent upon hybridization to target sequences. Together with hybrid-type [10] and multicomponent type molecular probes [11], these provide sensitive and direct means for genetic screening, biochip construction, biosensor development, and are used in many other applications [9]. All these approaches require covalent modification(s) of one or more oligonucleotides to carry different tags, for example organic dyes [12, 13], quantum dots [14], or gold nanoparticles [15, 16]. This results in increased cost and time needed for the analysis. To surmount this limitation, label-free detection strategies are being developed. Recently, several G-quadruplex based methods have been reported that specifically detect target DNA by peroxidase-mimicry of G-quadruplex DNA when bound to a porphyrin co-factor [17–21]. The use of unstable H<sub>2</sub>O<sub>2</sub> and porphyrin species can, however, negatively affect the reproducibility of analytical assays based on this system. In terms of stability and reproducibility, molecules with G-quadruplex-mediated fluorescence properties provide interesting new opportunities for label-free detection of nucleic acids [22–30].

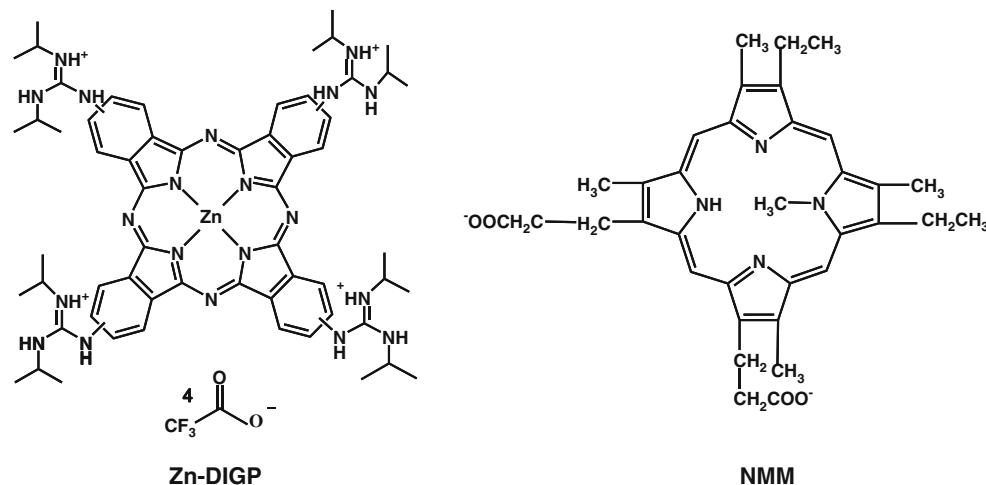
In recent years, several groups have demonstrated that the folding of split G-quadruplex sequences can be promoted by their hybridization to a DNA sequence that is complementary to the regions surrounding the G-quadruplex motif. As readout of hybridization and folding, Kolpashchikov used a split peroxidase DNAenzyme to visualize single nucleotide polymorphisms using a colorimetric assay [19]. To optimize the performance of such G-quadruplex-based sensors, Sintim and co-workers systematically studied the effect of the architectural features of G-rich DNA probes on the catalytic efficiency of self-assembling peroxidase-mimicking DNazymes [20]. Here we report a simple and sensitive hybridization probe based on small fluorescent molecules in a non-covalent complex

with a split G-quadruplex motif. This system might have significant advantages over peroxidase-based methods in terms of the sensitivity and simplicity provided by direct fluorescence readouts.

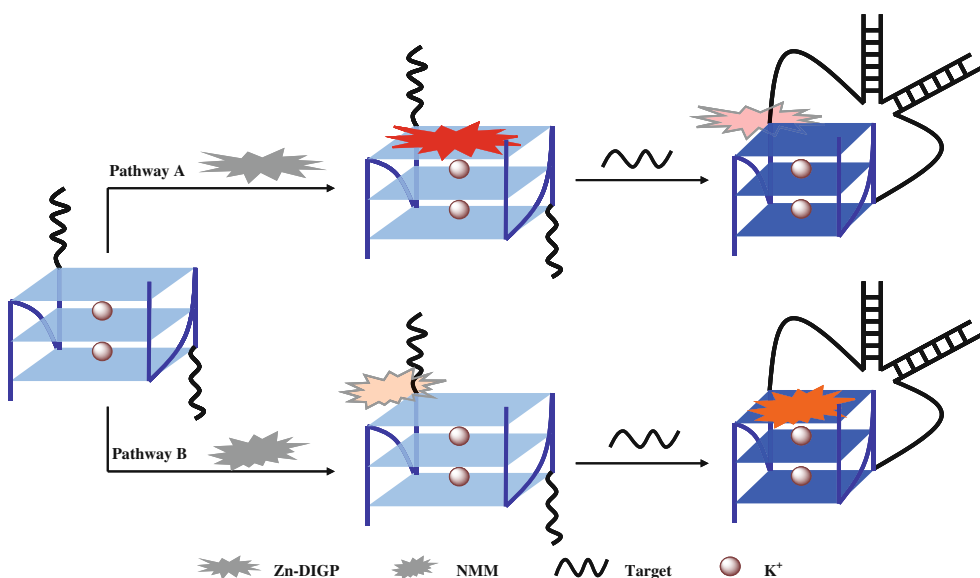
Small molecules with fluorescence properties sensitive to G-quadruplex folding are actively being developed as fluorescent probes and drug candidates. In this communication, we selected two probes (detailed structures are shown in Fig. 1) having different physicochemical properties that selectively bind G-quadruplex DNA. Bolton and co-workers reported that the anionic porphyrin derivative *N*-methylmesoporphyrin IX (NMM) had increased fluorescence on binding an intermolecular G-quadruplex formed by (GGGGTTTTGGGG)<sub>2</sub> [23]. More recently, Luedtke and co-workers reported a new cationic phthalocyanine derivative tetrakis(dicyclohexylguanidino)-zinc-phthalocyanine (Zn-DIGP) with high affinity for a quadruplex sequence derived from the c-Myc promoter (TGAGGGTGGG GAGGGTGGGAA) [22, 31].

In this study, we split the c-Myc G-quadruplex sequence into two fragments with flanking segments complementary to a target DNA sequence derived from the hepatitis B viral gene “HBV” (Scheme 1). In the presence of potassium ions, the two fragments assemble into a G-quadruplex structure that is stabilized, in part, by non-covalent interactions with the fluorescent probe itself [32]. Addition of complementary DNA to this solution further stabilizes the G-quadruplex structure while introducing conformational constraints into the complex. Hybridization therefore changes the local environment and fluorescence properties of each dye molecule. Interestingly, on DNA probe hybridization, fluorescence enhancement was observed for NMM whereas reduced fluorescence was observed for Zn-DIGP. In both cases the resulting changes in fluorescence emission enable sensitive, convenient, and label-free detection of mismatches between the probes and target DNA.

**Fig. 1** Structures of tetrakis (dicyclohexylguanidino)-zinc-phthalocyanine-TFA<sub>4</sub> (Zn-DIGP) and *N*-methylmesoporphyrin IX (NMM)



**Scheme 1** Schematic illustration of DNA sensors based on turn-off (*pathway A*) and turn-on (*pathway B*) fluorescence changes, utilizing split G-quadruplex probes. In the presence of  $K^+$ , a split c-Myc (blue) forms an associated G-quadruplex-fluorescent dye complex. Sequence-specific DNA hybridization results in reduced fluorescence from Zn-DIGP (*pathway A*) or increased fluorescence from NMM (*pathway B*)



## Experimental

### Reagents

HPLC-purified oligonucleotides without any modifications were obtained from Sangon Biotechnology (Shanghai, China) (Table 1 and Electronic Supplementary Material Table S1). Tetrakis(diisopropylguanidino)-zinc-phthalocyanine-TFA<sub>4</sub> salt (Zn-DIGP) was synthesized in accordance with published procedures [22]. *N*-Methylmesoporphyrin IX (NMM) was purchased from Frontier Scientific (Logan, Utah, USA). The oligonucleotides were dissolved in “TEK buffer” containing 50 mmol L<sup>-1</sup> Tris-HCl (pH 7.4) 0.5 mmol L<sup>-1</sup> EDTA, and 150 mmol L<sup>-1</sup> KCl, and were kept at -20 °C. DNA stock solutions were quantified using a Cary 500 UV-visible-NIR spectrometer (Varian). Stock solutions of Zn-DIGP (1 mmol L<sup>-1</sup>) and NMM (5 mmol L<sup>-1</sup>) were prepared in DMSO, stored in the dark at -20 °C, and diluted to the required concentration with aqueous TEK buffer. Double-distilled water was used throughout.

**Table 1** Sequences of split probes and target DNA

Split probes	Sequence (5' to 3')
PSa	GCAGACACATCCAGTTTGAGGGTGGG
PSb	AGGGTGGGAATTTCGATAGCCAGGACAA
PSc	GCAGACACATCCAGTGAGGGTGGG
PSd	AGGGTGGGAACGATAAGCCAGGACAA
CSab	GCAGACACATCCAGTTTGAGGGTGGG GGGTGGGAATTTCGATAGCCAGGACAA
Target	TTGTCTGGCTATCGCTGGATGTGCTGC

### Selecting the optimum split probes

We designed and tested four groups of split probes: PSa/PSb (1), PSa/PSd (2), PSc/PSb (3), and PSc/PSd (4) (Table 1). Each group or linked probe (CSab) was incubated with Zn-DIGP and HBV “Target” DNA in the presence of 150 mmol L<sup>-1</sup> KCl (pH 7.4) for 30 min at 20 °C and quantified by fluorescence (Ex 620 nm, Em 702 nm). Order of addition: 60 µL HBV target (1 µmol L<sup>-1</sup>), 60 µL of each split probe or CSab (2 µmol L<sup>-1</sup>), and 60 µL Zn-DIGP (10 µmol L<sup>-1</sup>) were mixed successively. The mixture was adjusted to 600 µL with TEK buffer, incubated for 30 min at 20 °C, and fluorescence spectra were collected on a Perkin–Elmer LS 55 luminescence spectrometer at 20 °C. Apparatus settings: slits 5/15 nm, scan rate 500 nm min<sup>-1</sup>, excitation at 620 nm and emission at 702 nm.

### Target DNA detection and control experiments

Titration of HBV with Zn-DIGP (or NMM) was conducted in the presence and absence of PSa/PSb. Generally, 600 µL TEK buffer solutions containing 1 µmol L<sup>-1</sup> Zn-DIGP or NMM, 200 nmol L<sup>-1</sup> of each split probe (PSa/PSb), and target DNA of different concentrations were incubated for 30 min at 20 °C. In the presence or absence of PSa/PSb, titrations of HBV with Zn-DIGP (or NMM) were also conducted. And fluorescence spectra of the Zn-DIGP plus Duplex DNAs composed of HBV and its complementary oligomer were acquired. The duplexes were prepared by heating the targets and complementary stands at 95 °C, cooling to room temperature, diluting with 600 µL buffer solution containing 1 µmol L<sup>-1</sup> Zn-DIGP or NMM to a final concentration of 100 nmol L<sup>-1</sup> duplexes (100 nmol L<sup>-1</sup>

target DNA and 100 nmol L<sup>-1</sup> complementary target DNA), and incubating for 30 min at 20 °C before collecting the fluorescence spectra. Apparatus settings for NMM were: slits 5/15 nm, scan rate 500 nm min<sup>-1</sup>, excitation at 399 nm and emission at 614 nm.

#### CD measurements

Circular dichroism (CD) spectra were collected using a Jasco J-810 spectropolarimeter (Tokyo, Japan) at 20 °C. CD measurements from 210 to 350 nm were taken, the data pitch was 0.1 nm, scan speed was 100 nm min<sup>-1</sup>, response time was 0.5 s, and bandwidth was 1 nm. Sample solutions containing 5 μmol L<sup>-1</sup> of each split probe (PSa/PSb), HBV targets (0, 2.5, or 5 μmol L<sup>-1</sup>), and dyes (10 μmol L<sup>-1</sup> Zn-DIGP or NMM) were incubated for 2 h, then the CD spectra were recorded. Each spectrum was collected by subtracting that of the CD buffer.

#### Evaluating specificity of both biosensors toward mismatched targets

Single-base, two-base, and four-base mismatched targets were designed to test specificity of target hybridization. The detailed sequences of these are shown in Table S1 in the Electronic Supplementary Material. Final concentrations of 1 μmol L<sup>-1</sup> Zn-DIGP or NMM, 200 nmol L<sup>-1</sup> of each split probe (PSa/PSb), 100 nmol L<sup>-1</sup> mismatched targets or 100 nmol L<sup>-1</sup> perfectly matched target were used for these experiments.

#### Applicability in the presence of biological fluids

To evaluate the possible application of our method in medical diagnostics, human serum and human urine were used. Fresh human serum was obtained from a local hospital, and fresh human urine was collected from a member of our laboratory. The serum and urine were centrifuged at 8000 rpm for 10 min to remove precipitates, and the supernatants were diluted 100-fold using TEK buffer and used in place of pure TEK buffer for sample preparation as described above. The resulting 600-μL solutions contained 1 μmol L<sup>-1</sup> Zn-DIGP or NMM, 200 nmol L<sup>-1</sup> of each split probe (PSa/PSb), HBV targets (50 nmol L<sup>-1</sup> for turn-off mode and 100 nmol L<sup>-1</sup> for turn-on mode) and 1% human serum or urine. All apparatus settings were the same as those described above.

## Results and discussion

Previous studies have demonstrated that the boundary architecture surrounding a G-quadruplex motif can affect hemin binding and catalytic activity [20]. We therefore

expected that the fluorescent changes due to G-quadruplex folding and target hybridization might also be sensitive to different boundary architecture. A significant reduction of fluorescence was observed compared with samples lacking the target DNA for each group split probe (compare black and red bars, Fig. 2). The reduction in fluorescence was 2.0, 1.9, 1.4, and 1.5-fold for groups 1–4, respectively. The introduction of four thymidine residues in the PSa/PSb probes therefore provided the greatest sensitivity to target hybridization. Interestingly, the relative quenching effect was fractionally larger for the PSa/PSb split probes compared with a control sequence (CSab, Table 1) that contained the same sequences as a single strand of DNA (Fig. 3).

Using the optimized split quadruplex probes PSa/PSb and Zn-DIGP we conducted titrations of the HBV target sequence. These titrations revealed a linear fluorescence response from 10 to 80 nmol L<sup>-1</sup> of HBV target DNA with a limit of detection (LOD) of 3.2 nmol L<sup>-1</sup> (*S/N*=3, *R*=0.994) (Fig. 4a and c). When similar titrations were conducted using NMM as the fluorescent probe, fluorescence intensity increases were observed, and a wider linear response range from 5–200 nmol L<sup>-1</sup> (*R*=0.996) (Fig. 4b and d) and LOD of 5.4 nmol L<sup>-1</sup> were obtained. Seven repeat measurements of 50 nmol L<sup>-1</sup> target DNA concentration for turn-off and turn-on sensors yielded RSD (relative standard deviation) of 3.2% and 2.6%, respectively. Control titrations conducted in the absence of the PSa/PSb split probes indicated some direct binding between Zn-DIGP and the HBV target DNA above 100 nmol L<sup>-1</sup> target DNA

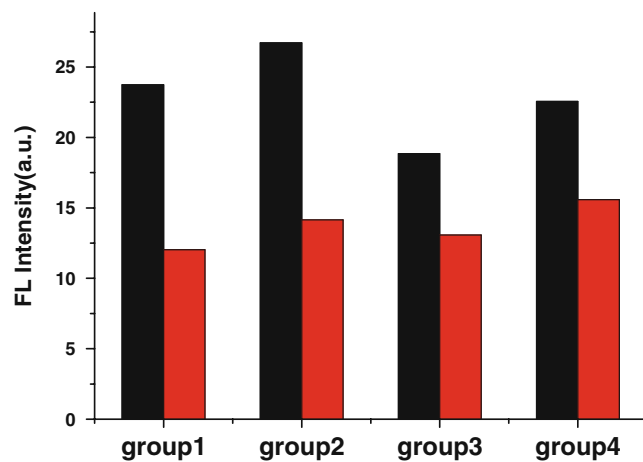


**Fig. 2** Selection of the optimum combination of split probes based on fluorescence quenching (pathway A). Groups 1 to 4 represent the combinations PSa/PSb, PSa/PSd, PSc/PSb and PSc/PSd, respectively. Black and red bars indicate fluorescence intensities in the absence and presence of HBV target DNA for each group. Experimental conditions: 1 μmol L<sup>-1</sup> Zn-DIGP, 200 nmol L<sup>-1</sup> of each split probe, and 100 nmol L<sup>-1</sup> HBV Target DNA in Tris-EDTA-potassium “TEK” buffer (pH 7.4)

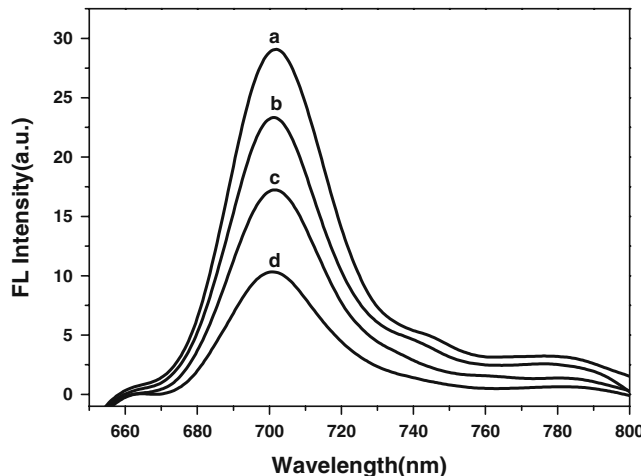
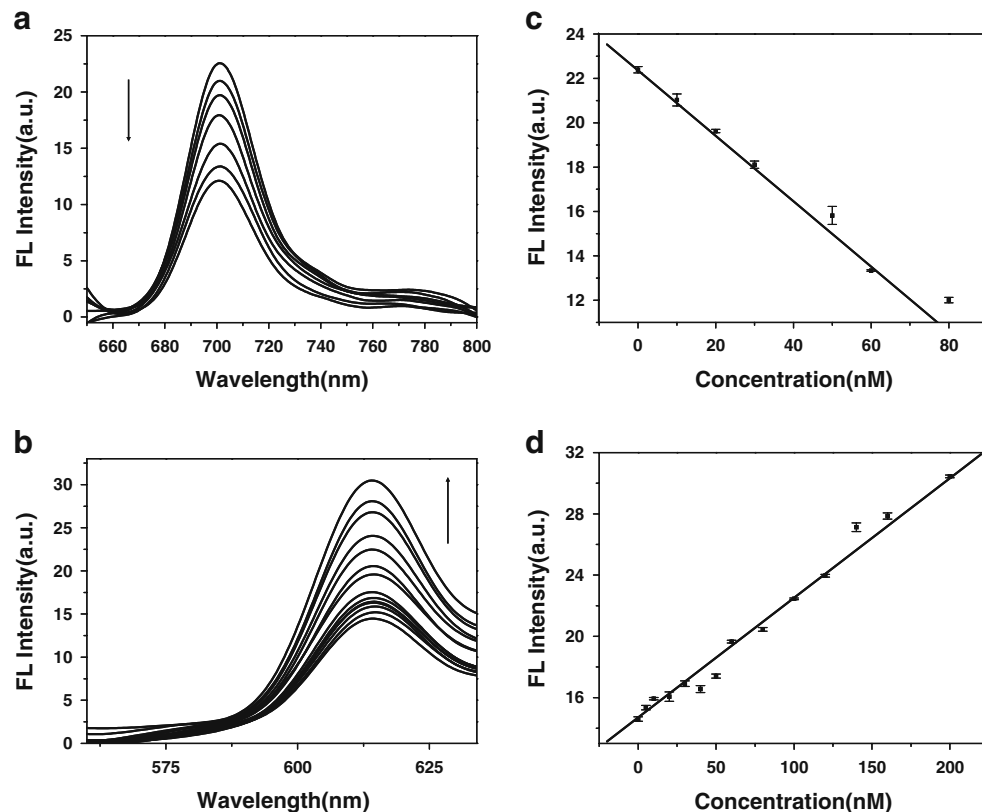


**Fig. 3** Fluorescence spectra of solutions containing Zn-DIGP and the linked probe CSab (*curve a*), plus target DNA (*curve b*), compared with the PSa/PSb split probes (*curve c*), plus target DNA (*curve d*). Experimental conditions:  $1 \mu\text{mol L}^{-1}$  Zn-DIGP,  $200 \text{ nmol L}^{-1}$  linked probe (CSab),  $200 \text{ nmol L}^{-1}$  of each split probe (PSa/PSb)  $\pm$   $100 \text{ nmol L}^{-1}$  HBV target DNA in TEK buffer (pH 7.4). Excitation = 620 nm

(Electronic Supplementary Material Fig. S1A). NMM, in contrast, did not bind directly to the single-stranded HBV target DNA through  $200 \text{ nmol L}^{-1}$  (Electronic Supplementary Material Fig. S1B).

**Fig. 4** Fluorescence response as a function of concentration of target DNA: 0, 10, 20, 30, 50, 60, and  $80 \text{ nmol L}^{-1}$  (**a** and **c**, Zn-DIGP); and 0, 5, 10, 20, 30, 40, 50, 60, 80, 100, 120, 140, 160, and  $200 \text{ nmol L}^{-1}$  (**b** and **d**, NMM). The error bars indicate the standard deviation of triplicate determinations for each concentration of target DNA. Experimental conditions:  $1 \mu\text{mol L}^{-1}$  Zn-DIGP (**a** and **c**) or NMM (**b** and **d**),  $200 \text{ nmol L}^{-1}$  of each split probe in TEK buffer (pH 7.4)



To evaluate the fluorescence signals originating from possible direct interactions between the fluorescent probes and duplex DNA, fluorescent spectra were measured for mixtures of duplex DNA and each dye molecule (Electronic Supplementary Material Fig. S2). The fluorescence intensity (curve 2) obtained from the mixture of duplex DNA and Zn-DIGP was only slightly higher than that obtained from Zn-DIGP alone (curves 1 and 2, Fig. S2A, Electronic Supplementary Material). This indicates little direct effect of the duplex DNA on the fluorescence enhancements observed in the presence of the split quadruplex probes. These results suggest that upon hybridization of the split probes to the HBV target DNA the fluorescence quenching of Zn-DIGP is because of conformational constraints rather than the formation of duplex DNA. Similarly, no fluorescence enhancement of NMM in the presence of duplex DNA was observed (Electronic Supplementary Material Fig. S2B). We therefore conclude that interactions between duplex DNA and these dye molecules do not interfere with this sensor strategy.

To characterize the global secondary structures of each complex, a series of CD spectra experiments were conducted. It has been reported that CD spectra of parallel G-quadruplex structures have a positive peak near 270 nm and a negative peak around 240 nm [33, 34]. Based on the CD curves in Fig. 5a in comparison with previous studies, we conclude

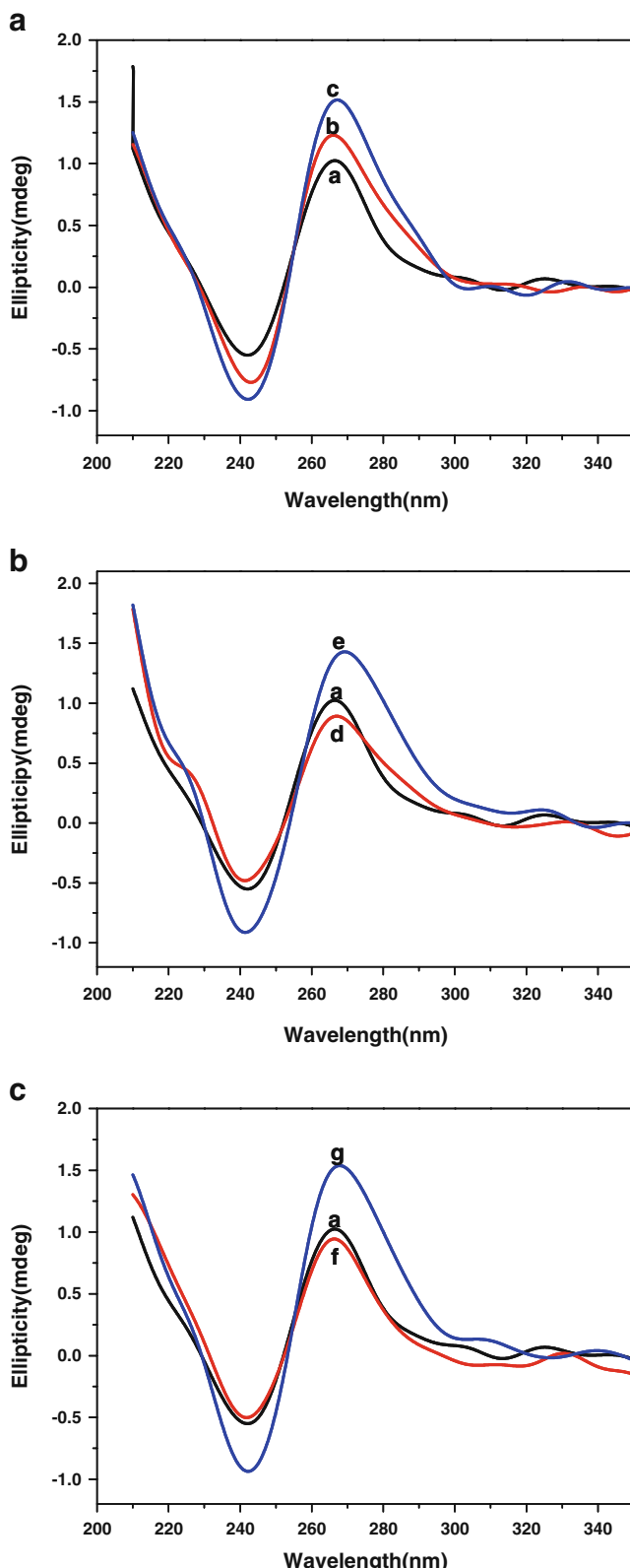


**Fig. 5** (a) CD spectra of split probes (PSa/PSb) with increasing concentrations of HBV (*a*, *b*, *c*), (b) CD spectra of split probes in the presence of Zn-DIGP (*d*) and Zn-DIGP plus HBV (*e*), (c) CD spectra of split probes in the presence of NMM (*f*) and NMM plus HBV (*g*). Experimental conditions: 0 nmol L<sup>-1</sup> (*a*, *d*, *f*), 2.5 μmol L<sup>-1</sup> (*b*), or 5 μmol L<sup>-1</sup> (*c*, *e*, *g*) HBV DNA, 10 μmol L<sup>-1</sup> Zn-DIGP or NMM, and 5 μmol L<sup>-1</sup> of each probe in TEK buffer (pH 7.4, 150 mmol L<sup>-1</sup> KCl)

that in the presence of potassium ions (“TEK” buffer) the split probes assemble into parallel G-quadruplexes (*curve a*). Upon addition of HBV target DNA, the values for the CD minimum and maximum increased in intensity, suggesting

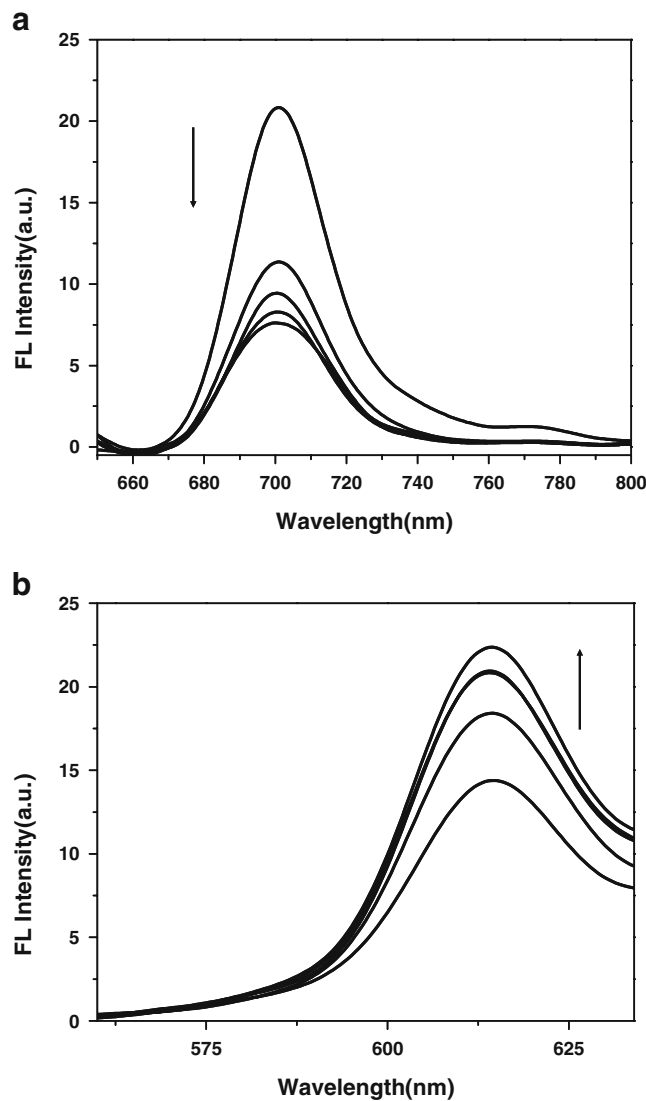


**Fig. 6** Fluorescence detection of mismatches using the split G-quadruplex approach. The arrows indicate the changes in complex emission for the split probes only, four-base mismatched, two-base mismatched, single-base mismatched and perfectly matched target DNA, respectively. Experimental conditions: 1 μmol L<sup>-1</sup> Zn-DIGP (**a**) or NMM (**b**), 200 nmol L<sup>-1</sup> of each split probe, 100 nmol L<sup>-1</sup> of perfectly matched or mismatched targets in TEK buffer (pH 7.4)

further stabilization of the G-quadruplex structure by added conformational constraints. To evaluate the potential effect of each added fluorescent probe, we took gathered CD data in the presence of Zn-DIGP (Fig. 5b) or NMM (Fig. 5c). In both cases, the enhanced CD signals were only observed upon addition of the target DNA. By comparing the trends observed by CD to those of fluorescence spectroscopy (Fig. 3a and b), we propose that the conformational constraints imposed on parallel G-quadruplex by target DNA might favor the binding interaction between G-quadruplex and NMM (leading to enhanced fluorescence), and disfavor the binding interaction between G-quadruplex and Zn-DIGP (leading to diminished fluorescence).

To test the specificity of the fluorescence readout resulting from hybridization, we prepared complexes containing zero, one, two, or four mismatches in the target sequence. For both fluorescent probes, fluorescence differences proportional to the number of mismatches present were observed (Fig. 6) [3]. In contrast to existing techniques based on other binary probes, our biosensors do not need to be modified with various tags. The sensitivity of our biosensors is comparable with that of traditional MBs [9, 35] and with that of colorimetric split G-quadruplex probes [18]. Further improvement is still possible if other G-quadruplex split modes and target sequences are used [18, 20, 21]. These results provide, to the best of our knowledge, the first examples of split-G-quadruplex systems using fluorescence as direct hybridization readout.

To evaluate the potential ability of these biosensors to function in complex mixtures of biological materials, we have evaluated both the turn-on (Zn-DIGP) and turn-off modes (NMM) in samples containing 1% human urine (Electronic Supplementary Material Table S2). Both types of biosensor functioned very well, and were able to report the presence of HBV target DNA with similar fluorescence changes as buffer-only samples. In the presence of 1% human serum, however, only the Zn-DIGP-containing probe remained functional. The NMM-based probe lost its functionality (Electronic Supplementary Material Table S2). This was probably because of tight binding of NMM to serum components.

## Conclusion

In summary, by using split probes we have successfully established a label-free method for nucleic acid detection by G-quadruplex mediated fluorescence. This split strategy is capable of detecting low concentrations of target DNA ( $3.2 \text{ nmol L}^{-1}$ ) and can discriminate between perfectly matched and mismatched DNA. The turn-off biosensor with Zn-DIGP was more sensitive, and could be used for analysis of serum-containing samples. Furthermore, we

have shown that conformational constraints have a significant effect on the properties of G-quadruplex. These results provide an important proof of principle for this approach and motivate further refinement of our system to detect single nucleotide polymorphisms.

**Acknowledgements** This work was supported by the National Natural Science Foundation of China (nos 20905056 and 20735003), the 973 Project (2009CB930100 and 2010CB933600), and the Swiss National Science Foundation (no. 130074).

## References

1. Qin WJ, Yim OS, Lai PS, Yung L-YL (2010) Dimeric gold nanoparticle assembly for detection and discrimination of single nucleotide mutation in Duchenne muscular dystrophy. *Biosens Bioelectron* 25(9):2021–2025
2. Song J, Li Z, Cheng Y, Liu C (2010) Self-aggregation of oligonucleotide-functionalized gold nanoparticles and its applications for highly sensitive detection of DNA. *Chem Commun* 46 (30):5548–5550
3. Zuo X, Xia F, Xiao Y, Plaxco KW (2010) Sensitive and selective amplified fluorescence DNA detection based on exonuclease III-aided target recycling. *J Am Chem Soc* 132(6):1816–1818
4. Hejazi MS, Pournaghi-Azar MH, Ahour F (2010) Electrochemical detection of short sequences of hepatitis C 3a virus using a peptide nucleic acid-assembled gold electrode. *Anal Biochem* 399 (1):118–124
5. Bonanni A, Pumera M, Miyahara Y (2010) Rapid, sensitive, and label-free impedimetric detection of a single-nucleotide polymorphism correlated to kidney disease. *Anal Chem*. doi:[10.1021/ac100165q](https://doi.org/10.1021/ac100165q)
6. Li H, Sun Z, Zhong W, Hao N, Xu D, Chen H-Y (2010) Ultrasensitive electrochemical detection for DNA arrays based on silver nanoparticle aggregates. *Anal Chem*. doi:[10.1021/ac101193e](https://doi.org/10.1021/ac101193e)
7. Guo W, Yuan J, Dong Q, Wang E (2009) Highly sequence-dependent formation of fluorescent silver nanoclusters in hybridized DNA duplexes for single nucleotide mutation identification. *J Am Chem Soc* 132(3):932–934
8. Tyagi S, Kramer FR (1996) Molecular beacons: probes that fluoresce upon hybridization. *Nat Biotechnol* 14(3):303–308
9. Wang K, Tang Z, Yang Chaoyong J, Kim Y, Fang X, Li W, Wu Y, Medley Colin D, Cao Z, Li J, Colon P, Lin H, Tan W (2009) Molecular engineering of DNA: molecular beacons. *Angew Chem Int Ed* 48(5):856–870
10. Yang CJ, Martinez K, Lin H, Tan W (2006) Hybrid molecular probe for nucleic acid analysis in biological samples. *J Am Chem Soc* 128(31):9986–9987
11. Grimes J, Gerasimova YV, Kolpashchikov DM (2010) Real-time SNP analysis in secondary-structure-folded nucleic acids. *Angew Chem Int Ed*. doi:[10.1002/anie.201004475](https://doi.org/10.1002/anie.201004475)
12. Häner R, Biner SM, Langenegger SM, Meng T, Malinovskii VL (2010) A highly sensitive, excimer-controlled molecular beacon. *Angew Chem Int Ed* 49(7):1227–1230
13. Yang CJ, Lin H, Tan W (2005) Molecular assembly of superquenchers in signaling molecular interactions. *J Am Chem Soc* 127(37):12772–12773
14. Zhang C-y, Hu J (2010) Single quantum dot-based nanosensor for multiple DNA detection. *Anal Chem*. doi:[10.1021/ac9026675](https://doi.org/10.1021/ac9026675)
15. Russ Algar W, Massey M, Krull UJ (2009) The application of quantum dots, gold nanoparticles and molecular switches to

- optical nucleic-acid diagnostics. *TrAC, Trends Anal Chem* 28 (3):292–306
- 16. Li H, Rothberg LJ (2004) DNA sequence detection using selective fluorescence quenching of tagged oligonucleotide probes by gold nanoparticles. *Anal Chem* 76(18):5414–5417
  - 17. Xiao Y, Pavlov V, Gill R, Bourenko T, Willner I (2004) Lighting up biochemiluminescence by the surface self-assembly of DNA–hemin complexes. *Chembiochem* 5(3):374–379
  - 18. Deng M, Zhang D, Zhou Y, Zhou X (2008) Highly effective colorimetric and visual detection of nucleic acids using an asymmetrically split peroxidase DNAzyme. *J Am Chem Soc* 130(39):13095–13102
  - 19. Kolpashchikov DM (2008) Split DNA enzyme for visual single nucleotide polymorphism typing. *J Am Chem Soc* 130(10):2934–2935
  - 20. Nakayama S, Sintim HO (2009) Colorimetric split G-quadruplex probes for nucleic acid sensing: improving reconstituted DNAzyme's catalytic efficiency via probe remodeling. *J Am Chem Soc* 131 (29):10320–10333
  - 21. Kolpashchikov DM (2010) Binary probes for nucleic acid analysis. *Chem Rev*. doi:[10.1021/cr900323b](https://doi.org/10.1021/cr900323b)
  - 22. Alzeer J, Vummidi Balayeshwanth R, Roth Phillip JC, Luedtke Nathan W (2009) Guanidinium-modified phthalocyanines as high-affinity G-quadruplex fluorescent probes and transcriptional regulators. *Angew Chem Int Ed* 48(49):9362–9365
  - 23. Arthanari H, Basu S, Kawano T, Bolton P (1998) Fluorescent dyes specific for quadruplex DNA. *Nucl Acids Res* 26(16):3724–3728
  - 24. White EW, Tanious F, Ismail MA, Reszka AP, Neidle S, Boykin DW, Wilson WD (2007) Structure-specific recognition of quadruplex DNA by organic cations: influence of shape, substituents and charge. *Biophys Chem* 126(1–3):140–153
  - 25. Yang Q, Xiang J, Yang S, Li Q, Zhou Q, Guan A, Zhang X, Zhang H, Tang Y, Xu G (2010) Verification of specific G-quadruplex structure by using a novel cyanine dye supramolecular assembly: II. The binding characterization with specific intramolecular G-quadruplex and the recognizing mechanism. *Nucl Acids Res* 38(3):1022–1033
  - 26. Yang Q, Xiang J, Yang S, Zhou Q, Li Q, Tang Y, Xu G (2009) Verification of specific G-quadruplex structure by using a novel cyanine dye supramolecular assembly: I. Recognizing mixed G-quadruplex in human telomeres. *Chem Commun* 9:1103–1105
  - 27. Ma D-L, Che C-M, Yan S-C (2009) Platinum(II) complexes with dipyridophenazine ligands as human telomerase inhibitors and luminescent probes for G-quadruplex DNA. *J Am Chem Soc* 131 (5):1835–1846
  - 28. Yang P, De Cian A, Teulade-Fichou M-P, Mergny J-L, Monchaud D (2009) Engineering bisquinolinium/thiazole orange conjugates for fluorescent sensing of G-quadruplex DNA13. *Angew Chem Int Ed* 48(12):2188–2191
  - 29. Koeppel F, Riou J-F, Laoui A, Mailliet P, Arimondo PB, Labit D, Petitgenet O, Helene C, Mergny J-L (2001) Ethidium derivatives bind to G-quartets, inhibit telomerase and act as fluorescent probes for quadruplexes. *Nucl Acids Res* 29(5):1087–1096
  - 30. Chang C-C, Kuo IC, Ling IF, Chen C-T, Chen H-C, Lou P-J, Lin J-J, Chang T-C (2004) Detection of quadruplex DNA structures in human telomeres by a fluorescent carbazole derivative. *Anal Chem* 76(15):4490–4494
  - 31. Phan AT, Modi YS, Patel DJ (2004) Propeller-type parallel-stranded G-quadruplexes in the human c-myc promoter. *J Am Chem Soc* 126(28):8710–8716
  - 32. Burge S, Parkinson GN, Hazel P, Todd AK, Neidle S (2006) Quadruplex DNA: sequence, topology and structure. *Nucl Acids Res* 34(19):5402–5415
  - 33. Seenivasay J, Rezler EM, Powell TJ, Tye D, Gokhale V, Joshi CS, Siddiqui-Jain A, Hurley LH (2004) The dynamic character of the G-quadruplex element in the c-MYC promoter and modification by TMPyP4. *J Am Chem Soc* 126(28):8702–8709
  - 34. Qin Y, Hurley LH (2008) Structures, folding patterns, and functions of intramolecular DNA G-quadruplexes found in eukaryotic promoter regions. *Biochimie* 90(8):1149–1171
  - 35. Venkatesan N, Jun Seo Y, Hyean Kim B (2008) Quencher-free molecular beacons: a new strategy in fluorescence based nucleic acid analysis. *Chem Soc Rev* 37(4):648–663